

# First-principles investigation of intrinsic defects and (N, O) impurity atom stimulated Al vacancy in $\text{Ti}_2\text{AlC}$

Ting Liao, Jingyang Wang', and Yanchun Zhou

Citation: [Appl. Phys. Lett.](#) **93**, 261911 (2008); doi: 10.1063/1.3058718

View online: <http://dx.doi.org/10.1063/1.3058718>

View Table of Contents: <http://aip.scitation.org/toc/apl/93/26>

Published by the [American Institute of Physics](#)

---

---



**FIND THE NEEDLE IN THE  
HIRING HAYSTACK**

POST JOBS AND REACH THOUSANDS OF  
QUALIFIED SCIENTISTS EACH MONTH.

PHYSICS TODAY | JOBS  
[WWW.PHYSICSTODAY.ORG/JOBS](http://WWW.PHYSICSTODAY.ORG/JOBS)

# First-principles investigation of intrinsic defects and (N, O) impurity atom stimulated Al vacancy in $\text{Ti}_2\text{AlC}$

Ting Liao,<sup>1,2</sup> Jingyang Wang,<sup>1,a)</sup> and Yanchun Zhou<sup>1</sup>

<sup>1</sup>Shenyang National Laboratory for Materials Science, Institute of Metal Research, Chinese Academy of Sciences, Shenyang 110016, China

<sup>2</sup>Graduate School, Chinese Academy of Sciences, Beijing 100039, China

(Received 28 October 2008; accepted 4 December 2008; published online 31 December 2008)

We use first-principles calculations to study the energetics of intrinsic defects in  $\text{Ti}_2\text{AlC}$  and the effect of N or O impurity atoms on the generation of Al vacancies. The insertion of impurity atoms lowers the vacancy formation energy of its neighboring Al. The formation of Al vacancies is related to the experimental observations of growth of AlN or  $\text{Al}_2\text{O}_3$  nanowires and nanofibers on the surface of  $\text{Ti}_2\text{AlC}$ . Since the growth of these nanostructures is controlled by the generation and migration of intrinsic defects, we propose that a tunable method for synthesis of such nanostructures is possible by controlling impurities. © 2008 American Institute of Physics.

[DOI: 10.1063/1.3058718]

A tunable method for generating nanoscale binary nitrides or oxides on the surface of  $M_{n+1}AX_n$  phases (where  $M$  is an early transition metal,  $A$  is an A-group element, and  $X$  is carbon and/or nitrogen) is attainable in desired exterior atmosphere via the mechanism of combination of escaped A-group element and ambient atom. Scanning electron microscopy and transmission electron microscopy studies have shown appreciable amount of binary compounds formed on the surface of  $MAX$  phases during high-temperature treatment.<sup>1–4</sup> For example, single-crystalline AlN in hexagonal wurtzite structure and  $\text{Al}_2\text{O}_3$  nanowires have been synthesized by the nitridation of  $\text{Ti}_3\text{Si}_{0.9}\text{Al}_{0.1}\text{C}_2$  solid solution;<sup>1</sup> silica nanofiber has been formed on the fracture surfaces of  $\text{Ti}_3\text{SiC}_2$  after creep failure.<sup>2</sup> Most importantly, the characteristic crystal structure of  $MAX$  phase is still maintained with either A-group atoms depletion or substantial impurity atom present originating from residual gas or solid phase reactions.<sup>5–8</sup> It implies that  $MAX$  phases can serve as stable source for producing desirable binary nitrides or oxides in nanoscale. Inspired by the highly anisotropic hexagonal crystal structure of  $MAX$  phases, wherein slabs of nonstoichiometric transition metal carbides are weakly coupled by atomic planes of A-group element, the nanoscale compound formation can be better understood by a constrained two-dimensional nanoscale free path for A-element atom passage. What is more interesting, some typical  $MAX$  phases, such as  $\text{Cr}_2\text{GaN}$  and  $\text{Zr}_2\text{InC}$ , can also extrude A-element filaments at room temperature.<sup>9,10</sup> If desirable nitrogen atmosphere is provided, it is of great possibility that high-quality technologically important GaN or InN material in nanoscale can be obtained. These phenomena suggest that a tunable method for producing nanoscale nitrides or oxides, whose growth should be controlled by the generation and migration of intrinsic defects, as well as appropriate chemical environment change, is possible. A deeper knowledge of interaction between impurity atom and point defects in  $MAX$  phases is thus technologically crucial for the production of desirable nanoscale materials by tuning ambient environments.

The special interest on  $\text{Ti}_2\text{AlC}$  originates from the fact that it is a serious candidate for a number of practical applications. In this letter, we investigate all possible intrinsic point defects, i.e., antisite, interstitial, and Frenkel pair in  $\text{Ti}_2\text{AlC}$ , and study the role of chemical potential using *ab initio* density functional theory. Then a formalism based on thermodynamical equilibrium consideration of  $\text{Ti}_2\text{AlC}$  with (N, O) impurity solubility and a given AlN or  $\text{Al}_2\text{O}_3$  is established to explain the promoted effects of these impurity atoms on the generation of Al vacancy in  $\text{Ti}_2\text{AlC}$ .

We have adopted a defect-in-supercell model based on the first-principles calculations. This was implemented using the CASTEP code.<sup>11</sup> The calculations were performed in a plane-wave basis, using fully nonlocal Vanderbilt-type ultrasoft pseudopotentials to describe the electron-ion interaction.<sup>12</sup> Exchange and correlation were treated by the Perdew–Wang functional,<sup>13</sup> adding a nonlocal correction in the form of the generalized gradient approximation. The energy cutoff for the plane-wave basis set used throughout this work was 550 eV for atomic and cell relaxations. Brillouin zone sampling was performed using the Monkhorst–Pack scheme.<sup>14</sup> We employed 32 atoms for single defect calculation and 72 atoms for defect cluster, which were in accord with  $2 \times 2 \times 1$  and  $3 \times 3 \times 1$  supercells.

The open-spaced region in  $\text{Ti}_2\text{AlC}$ , as highlighted by gray colors in Fig. 1(a), accommodates almost all intrinsic

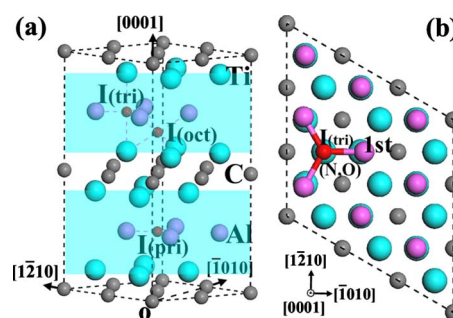


FIG. 1. (Color online) (a) Starting configurations of possible interstitial sites (as the smallest balls) in  $\text{Ti}_2\text{AlC}$ . Gray regimes illustrate the open-spaced region. (b) Configurations of Al atom first-nearest neighboring to the inserted impurity interstitials of N and O in  $\text{Ti}_2\text{AlC}$  supercell.

<sup>a)</sup>Electronic mail: jywang@imr.ac.cn.

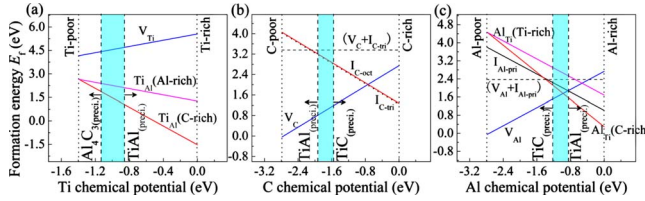


FIG. 2. (Color online) Different defect formation energies plotted with respect to the chemical potential of each component in  $\text{Ti}_2\text{AlC}$ . In each diagram, the gray region shows the stable region of pure  $\text{Ti}_2\text{AlC}$ , and the arrow indicates the chemical potential region for secondary bulk phase precipitation.

defects. The high-symmetry interstitial sites are modeled as the smallest atoms. In the Al atomic layer, interstitial site  $I_{(\text{tri})}$  is in the center of a bitriangular pyramid with Ti atom on the vertex, whereas  $I_{(\text{pri})}$  is encompassed by two Ti hexagonal rings of the lower and upper basal plane. Another high-symmetry interstitial site  $I_{(\text{oct})}$  can be characterized by an octahedron surrounded by three Al and three Ti atoms. A Frenkel defect is formed by moving an atom from its lattice site to the neighboring interstice. We generate Frenkel defects only for Al and C species with smaller radii. For antisite, we study two cases of Ti atom substituting on Al site and in the reverse, we do not substitute Ti or Al atom on C sites due to the large electronegative difference and vice versa.

The stability of defective structure usually depends on the environmental variables, and chemical potential analysis is employed here to compare the stability of defect structures as a function of environmental conditions.<sup>15,16</sup> The formation energy of each defect in  $\text{Ti}_2\text{AlC}$  can be defined as

$$E_f = E(n_{\text{Ti}}, n_{\text{Al}}, n_{\text{C}}) - n_{\text{Ti}}\mu_{\text{Ti}} - n_{\text{Al}}\mu_{\text{Al}} - n_{\text{C}}\mu_{\text{C}}, \quad (1)$$

where  $E(n_{\text{Ti}}, n_{\text{Al}}, n_{\text{C}})$  is the total energy of a supercell containing the defect and  $n_i$  and  $\mu_i$ , respectively, are the numbers of host atoms and the reference state chemical potential of each species. To avoid precipitation of elemental solids, the atomic chemical potentials should be smaller than that of the corresponding elemental solid. Denoting  $\Delta\mu_i = \mu_i - \mu_i^{\text{solid}}$  we thus have

$$\Delta\mu_{\text{Ti}} \leq 0, \quad \Delta\mu_{\text{Al}} \leq 0, \quad \Delta\mu_{\text{C}} \leq 0. \quad (2)$$

To maintain a stable  $\text{Ti}_2\text{AlC}$  compound at equilibrium condition, it is also required

$$\Delta E_f(\text{Ti}_2\text{AlC}) = 2\Delta\mu_{\text{Ti}} + \Delta\mu_{\text{Al}} + \Delta\mu_{\text{C}}, \quad (3)$$

where  $\Delta E_f(\text{Ti}_2\text{AlC})$  is the heat of formation of bulk  $\text{Ti}_2\text{AlC}$ . Equations (2) and (3) limit the chemical potentials in the triangle with vertices decided by  $(\Delta\mu_{\text{Ti}}, \Delta\mu_{\text{Al}}, \Delta\mu_{\text{C}})$ . For visual simplicity and easy comparison for defect species, each bound line of triangle is chosen to illustrate the dependence of formation energy on respective chemical potential of each component in Fig. 2.

If precipitation of binary compounds such as  $\text{Al}_4\text{C}_3$ ,  $\text{TiC}$ , and  $\text{TiAl}$  is considered, possible chemical potential for stable  $\text{Ti}_2\text{AlC}$  changes to narrow bounds, as shown by the gray zones in Fig. 2. The arrows indicate outer regions for binary bound phases. For example, in Fig. 2(a) whose formation energy changes as function of Ti chemical potential, away from the gray zone,  $\text{TiAl}$  will appear with

increment in Ti chemical potential and  $\text{Al}_4\text{C}_3$  will be present if Ti chemical potential goes beyond the reverse border.

In Fig. 2, the calculated results for intrinsic defects such as interstitials and antisites, as well as Frenkel pairs, under different chemical environments are displayed. The result for vacancy has been reported before<sup>6</sup> and is also displayed here for a better comparison. As can be noticed from Fig. 2(a), Ti vacancy is recognized as the most unlikely defect species for every available chemical potential, whereas the formation energy for antisite  $\text{Ti}_{\text{Al}}$  is quite low and has a negative value in (Ti- and C-rich) environment in particular. It is suggested that energy gain can be achieved on substituting Ti atom on Al lattice site. It is apparent from Fig. 2(b) that in C-rich environment, extra C atom can be accommodated almost equally in two interstitial sites [ $E_f(I_{\text{C-tri}})$  is only 0.035 eV lower than  $E_f(I_{\text{C-oct}})$ ]. Figure 2(c) shows that in Al-rich environment, Al disorder is preferred by either incorporating Al atom in open interstice ( $I_{\text{Al-pri}}$ ) or substituting Al on Ti sites depending on the relative abundance of carbon vacancy. In detail, aluminum interstitials will dominate when carbon vacancies are in excess, whereas antisite  $\text{Al}_{\text{Ti}}$  will be more energetically favorable in C-rich environment. Independent of the chemical potential of the surrounding reservoir, Al/C Frenkel pair is metastable defect cluster with relatively high formation energy of about 2.4 and 3.2 eV, respectively.

Small impurity atom, such as N or O, associated with natural atmosphere is known to be able to permeate into  $\text{Ti}_2\text{AlC}$  bulk materials<sup>5</sup> and is able to strongly affect the behavior of intrinsic defects due to chemical environment changes. The most favorably occupied interstice for N/O atoms is  $I_{\text{N/O-tri}}$ , whose formation energies are 0.8 and 1.2 eV, respectively, lower than the counterparts for  $I_{\text{N/O-oct}}$ . As shown in Fig. 1(b), the removed Al atom is chosen first-nearest neighbor to the inserted impurity atom.

To make the calculations tractable we consider the condition of practical interest, in which case Al-based binary compound does form. That is, we have thermal equilibrium between impurity-atom involved  $\text{Ti}_2\text{AlC}$  and Al-based binary compound,  $\text{Al}_2\text{O}_3$  or  $\text{AlN}$ . Equality of the chemical potential of Al atom in coexisting defective  $\text{Ti}_2\text{AlC}$  structure and precipitate  $\text{Al}_2\text{O}_3$  or  $\text{AlN}$  then requires

$$\mu_{\text{Al}}^{(\text{N/O})\text{-involved-Ti}_2\text{AlC}} = \mu_{\text{Al}}^{\text{AlN/Al}_2\text{O}_3}. \quad (4)$$

The defect formation energy in this case is then calculated by

$$E_f = E(n_{\text{Ti}}, n_{\text{Al}}, n_{\text{C}}, \text{N}) - n_{\text{Ti}}\mu_{\text{Ti}} - n_{\text{C}}\mu_{\text{C}} - (1 - n_{\text{Al}})\mu_{\text{N}} - n_{\text{Al}}\mu_{\text{AlN}} \quad (5)$$

or

$$E_f = E(n_{\text{Ti}}, n_{\text{Al}}, n_{\text{C}}, \text{O}) - n_{\text{Ti}}\mu_{\text{Ti}} - n_{\text{C}}\mu_{\text{C}} - (1 - 3/2n_{\text{Al}})\mu_{\text{O}} - 1/2n_{\text{Al}}\mu_{\text{Al}_2\text{O}_3}.$$

The composition gradients for the gas phases,  $\text{N}_2$  and  $\text{O}_2$ , through the scale can be better understood at this time by the induced internal gas pressure gradients, which in turn strongly influence microstructure development. We assumed an ideal gas behavior of nitrogen and oxygen, and their chemical potential can be referenced at  $(T=0, p=0)$  condition to one half of the total energy of the molecule  $\mu_{\text{N/O}}(T=0, p=0) = \frac{1}{2}E_{\text{N}_2/\text{O}_2}^{\text{total}}$ . Then the chemical potential was calculated using the well-known thermodynamic expression for ideal gases,



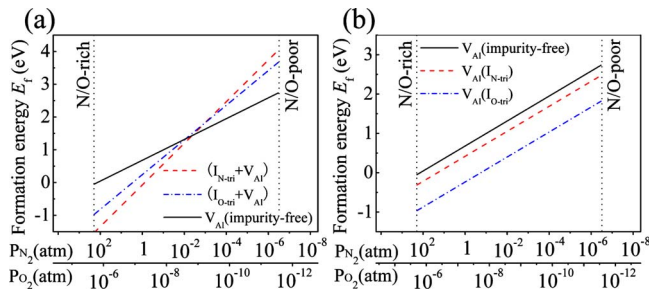


FIG. 3. (Color online) (a) Formation energy of Al vacancy and  $(V_{Al} + I_{N/O-tri})$  ( $i=N$  and  $O$ ) clusters as a function of pressure scale of ideal  $N_2$  and  $O_2$  gases at a fixed temperature of 1600 K. (b) Relative formation energy of Al vacancy for the impurity-free or impurity-involved crystal structures in the same scale.

$$\mu_{N/O}(T, p) = \mu_{N/O}(T, p^0) + 1/2kT \ln(p_{N_2/O_2}/p_{N_2/O_2}^0) \quad (6)$$

in which  $p^0$  is the pressure of reference state. The temperature dependence of the chemical potentials  $\mu(T, p^0)$  at the reference pressure  $p^0$  can be taken from thermochemical reference tables.<sup>17</sup>

In Fig. 3(a) we show the results of the formation energy of  $(I_{N/O-tri} + V_{Al})$  clusters for given Al-involved phases using the above equations, as well as that of single Al vacancy for comparison. As seen in Fig. 3(a), the formation energy of clusters is lower than that of single Al vacancy in high gas pressure condition but higher in low gas pressure condition. The negative formation energies of  $(I_{N/O-tri} + V_{Al})$  clusters in high pressure conditions indicate that Al atoms removal can occur spontaneously when N or O atom is incorporated into  $Ti_2AlC$  bulk, but when pressure is low, this phenomenon will be dramatically suppressed. However, we are more concerned about the stability of Al vacancy when impurity atoms have already been incorporated in  $Ti_2AlC$ , and in next we consider the relative stability of Al vacancy in  $(I_{N/O-tri} + V_{Al})$  clusters using the formation energies of  $I_O$  and  $I_N$ , respectively, as the reference states. It is clear from Fig. 3(b) that relative lower energy cost for impurity-induced  $V_{Al}$  than for pure one in full pressure range is noted, i.e., the presence of impurity atoms leads to obviously reduced formation energies of Al vacancy. It is suggested that once  $Ti_2AlC$  matrix accommodates a certain number of N/O impurity atoms, formation of Al vacancy will be promoted regardless of the environmental condition. Escaped Al atoms can easily combine with outer atmosphere to form binary nanostructures on the surface of  $Ti_2AlC$  matrixes. From Fig. 3(b), the effect of speeding up the escape of Al atoms from the lattice is more efficient for oxygen noted as a much lower Al vacancy formation energy at a relatively lower oxygen pressure compared to the case of nitrogen. This result can provide some thermodynamic reasons that Al atoms show a higher activity when combined with oxygen than nitrogen, and it also gives a hint to the experimental observed phenomena that AlN are formed as fine wires while  $Al_2O_3$  as coarse ones.<sup>1</sup>

The underlying physical origin of the effects of N/O impurity atoms on Al depletion is studied by examining the electron density isosurface of the defect-free structure and that after N/O impurity atom insertion. Two main characters are noticed in here. First, the addition of small impurity atom

on interstitial sites obtains valence electrons from its first-nearest-neighboring Al atoms, and obvious electron depletion is observed on the Al sites. Second, such valence electron transfer results in weakening of neighboring Ti–Al bond, which is demonstrated by less electron density populating within the neighboring Ti–Al bond. Hence, the appearance of impurity atom lowers the vacancy formation energy of Al atom and accelerates the removal of Al atom.

In conclusion, our work provides a quantitative assessment of the stability of different defect species, interstitial, antisite, and Frenkel pair in  $Ti_2AlC$  under different chemical conditions by using density-functional theory. Open-spaced region between compact TiC slabs in  $Ti_2AlC$  is capable of accommodating a number of defect species.  $Ti_{Al}/Al_{Ti}$  antisite shows extraordinary stability depending on desirable chemical environments; Al and C atoms with small atomic sizes can occupy various interstices of high symmetry. More intriguingly, impurity atoms associated with practical atmosphere, such as N and O, can be easily incorporated in  $Ti_2AlC$  matrix, and of primary importance, inserted N or O atom obviously weakens the bonding strength of neighboring Ti–Al bond and hence promotes the formation of Al vacancy. This result provides an underlying chemical and electronic origin for easier formation of Al vacancy, which facilitates the formation of nanoscale AlN or  $Al_2O_3$  wires in high-temperature treatment of  $Ti_2AlC$ . We propose, by appropriately tuning chemical atmosphere, technologically important materials, namely, A-group element involved nitrides or oxides, can be obtained from specific MAX phases.

This work was supported by the National Outstanding Young Scientist Foundation for Y.C.Z. and by the Natural Sciences Foundation of China under Grant Nos. 50832008 and 50672102.

- <sup>1</sup>H. B. Zhang, J. Zhang, Y. C. Zhou, Y. W. Bao, and M. S. Li, *J. Mater. Res.* **22**, 561 (2007).
- <sup>2</sup>Z. M. Sun, T. J. Zhen, and M. W. Barsoum, *J. Mater. Res.* **20**, 2895 (2005).
- <sup>3</sup>X. H. Wang and Y. C. Zhou, *Oxid. Met.* **59**, 303 (2003).
- <sup>4</sup>Z. J. Lin, M. J. Zhuo, Y. C. Zhou, M. S. Li, and J. Y. Wang, *J. Am. Ceram. Soc.* **89**, 2964 (2006).
- <sup>5</sup>J. Rosen, P. O. Å. Persson, M. Ionescu, A. Kondyurin, D. R. Mckenzie, and M. M. M. Bilek, *Appl. Phys. Lett.* **92**, 064102 (2008).
- <sup>6</sup>T. Liao, J. Y. Wang, and Y. C. Zhou, *Scr. Mater.* **59**, 854 (2008).
- <sup>7</sup>O. Wilhelmsson, J.-P. Palmquist, E. Lewin, J. Emmerlich, P. Eklund, P. O. Å. Persson, H. Höglberg, S. Li, R. Ahuja, O. Eriksson, L. Hultman, and U. Jansson, *J. Cryst. Growth* **291**, 290 (2006).
- <sup>8</sup>P. O. Å. Persson, J. Rosen, D. R. Mckenzie, M. M. M. Bilek, and C. Höglund, *J. Appl. Phys.* **103**, 066102 (2008).
- <sup>9</sup>M. W. Barsoum and L. Farber, *Science* **284**, 937 (1999).
- <sup>10</sup>M. W. Barsoum, E. N. Hoffman, R. D. Doherty, S. Gupta, and A. Zavalangos, *Phys. Rev. Lett.* **93**, 206104 (2004).
- <sup>11</sup>M. D. Segall, P. L. D. Lindan, M. J. Probert, C. J. Pickard, P. J. Hasnip, S. J. Clark, and M. C. Payne, *J. Phys.: Condens. Matter* **14**, 2717 (2002).
- <sup>12</sup>D. Vanderbilt, *Phys. Rev. B* **41**, 7892 (1990).
- <sup>13</sup>J. P. Perdew, J. A. Chevary, S. H. Vosko, K. A. Jackson, M. R. Pederson, D. J. Singh, and C. Fiolhais, *Phys. Rev. B* **46**, 6671 (1992).
- <sup>14</sup>J. D. Pack and H. J. Monkhorst, *Phys. Rev. B* **16**, 1748 (1977).
- <sup>15</sup>S. B. Zhang and J. E. Northrup, *Phys. Rev. Lett.* **67**, 2339 (1991).
- <sup>16</sup>A. S. Foster, F. L. Gejo, A. L. Shluger, and R. M. Nieminen, *Phys. Rev. B* **65**, 174117 (2002).
- <sup>17</sup>JANAF Thermochemical Tables, 2nd ed., edited by D. R. Stull and H. Prophet (U.S. National Bureau of Standards, Washington, D.C., 1971).